



Title: Pressure generation to 65 GPa in a Kawai-type multi-anvil apparatus with tungsten carbide anvils  
Author: Takayuki Ishii, Daisuke Yamazaki, Noriyoshi Tsujino, Fang Xu, Zhaodong Liu, Takaaki Kawazoe, Takafumi Yamamoto, Dmitry Druzhbin, Lin Wang, Yuji Higo, Yoshinori Tange, Takashi Yoshino, Tomoo Katsura  
Publication: High Pressure Research  
Publisher: Taylor & Francis  
Date: 14 Sep 2017

This is an Accepted Manuscript of an article published by Taylor & Francis in High Pressure Research on 14 Sep 2017, available online:  
<https://doi.org/10.1080/08957959.2017.1375491>

1 **Pressure generation to 65 GPa in Kawai-type multi-anvil apparatus with tungsten**  
2 **carbide anvils**

3  
4 Takayuki Ishii<sup>a\*</sup>, Daisuke Yamazaki<sup>b</sup>, Noriyoshi Tsujino<sup>b</sup>, Fang Xu<sup>b</sup>, Zhaodong Liu<sup>a</sup>,  
5 Takaaki Kawazoe<sup>a</sup>, Takafumi Yamamoto<sup>c</sup>, Dmitry Druzhbin<sup>a</sup>, Lin Wang<sup>a</sup>, Yuji Higo<sup>d</sup>,  
6 Yoshinori Tange<sup>d</sup>, Takashi Yoshino<sup>b</sup>, and Tomoo Katsura<sup>a</sup>

7  
8 <sup>a</sup>*Bayerisches Geoinstitut, University of Bayreuth, 95440 Bayreuth, Germany*

9 <sup>b</sup>*Institute for Study of the Earth's Interior, Okayama University, Misasa, 682-0193*  
10 *Japan*

11 <sup>c</sup>*Department of Earth and Planetary systems sciences, Graduate School of Science,*  
12 *Hiroshima University, Kagamiyama 1-3-1, Higashi-Hiroshima, 739-8526 Japan*

13 <sup>d</sup>*Japan Synchrotron Radiation Research Institute (JASRI), 1-1-1, Kouto, Sayo-cho,*  
14 *Sayo-gun, Hyogo 679-5198 Japan*

15  
16 \*Corresponding author. Email address: [Takayuki.ishii@uni-bayreuth.de](mailto:Takayuki.ishii@uni-bayreuth.de)

35 **Pressure generation to 65 GPa in Kawai-type multi-anvil apparatus with tungsten**  
36 **carbide anvils**

37

38 We have expanded the pressure ranges at room and high temperatures  
39 generated in a Kawai-type multi-anvil apparatus (KMA) using tungsten carbide (WC)  
40 anvils with a high hardness of  $H_v = 2700$  and a Young's modulus of 660 GPa. At room  
41 temperature, a pressure of 64 GPa, which is the highest pressure generated with KMA  
42 using WC anvils in the world, was achieved using  $1^\circ$ -tapered anvils with a 1.5-mm  
43 truncation. Pressures of 48-50 GPa were generated at high temperatures of 1600 to 2000  
44 K, which are also higher than previously achieved. Tapered anvils make wide anvil gaps  
45 enabling efficient X-ray diffraction. The present pressure generation technique can be  
46 used for studying the upper part of the Earth's lower mantle down to 1200 km depth  
47 without sintered diamond anvils.

48

49 **Keywords:** Kawai-type multi-anvil apparatus; tungsten carbide anvil; sintered diamond  
50 anvil; synchrotron; lower mantle

51

52 **1. Introduction**

53 The Kawai-type multi-anvil apparatus (KMA) is one of the most popular high-  
54 pressure apparatus in the field of deep-Earth science, which adopts the 6-8-type double-  
55 stage compression system [1]. The KMA is one type of multi-anvil apparatus which is  
56 characterized by the double-stage compression such that an octahedral pressure medium  
57 is squeezed by truncated corners of eight cubic anvils which are compressed by six  
58 outer anvils. Main advantages of KMAs are relatively large volumes, high pressures and  
59 homogeneous  $P$ - $T$  distributions in samples. For example, KMAs have by  $\sim 1000$  times  
60 larger sample volumes than diamond anvil cells under similar pressure conditions.  
61 Because of these advantages, KMAs have been especially used for precisely  
62 determining mantle mineralogy and measuring physical properties of minerals.

63 Second-stage anvils of KMAs are usually made of tungsten carbide (WC), but  
64 sintered diamond (SD) is sometimes employed to generate higher pressures. KMAs  
65 with conventional WC anvils, whose hardness and Young's modulus are about  $H_v =$   
66 1800 and 560 GPa, respectively, can generate pressures up to 25 GPa [e.g. 2],  
67 corresponding to the uppermost part of the lower mantle down to 700 km depth. On the  
68 other hand, pressures up to 60 GPa were routinely generated by using SD anvils [e.g. 3-

69 5], and pressures over 100 GPa were attained by using the latest techniques [6].  
70 However, SD anvils are much more expensive than WC anvils. Moreover, special  
71 manufacturing techniques for processing anvils and parts of pressure cells are necessary  
72 for successful high-pressure and -temperature generation. As a result, SD anvils can be  
73 used by only limited research groups [7,8]. For these reasons, it is desired to expand the  
74 pressure range of KMAs with WC anvils.

75         Recently, pressures over 40 GPa were achieved at both room temperature and  
76 high temperature of 2000 K even using WC anvils in combination with sophisticated  
77 high-pressure techniques [9]. The most essential point in this high-pressure generation is  
78 use of hard WC, TF05 produced by Fuji Die Co. Ltd., whose hardness and Young's  
79 modulus are  $H_v = 2200$  and 610 GPa, respectively. Another important point is tapering  
80 of the second-stage anvils, which allows higher pressure generation by making more  
81 stress concentration to anvil top [9]. In addition to Ishii et al. [9], pressures close to 50  
82 GPa were generated by using even harder WC anvils without anvil tapering (TJS01,  $H_v$   
83 = 2700 and Young's modulus = 660 GPa), which were newly developed also by Fuji Die  
84 Co., Ltd. [10]. However, Kunimoto et al. [10] conducted the pressure generation test  
85 only at room temperature. For application to deep-Earth science, simultaneous  
86 generation of high-pressure and high-temperature conditions is crucial. Additionally,  
87 Kunimoto et al. [10] conducted the pressure generation tests at press loads only up to 10  
88 MN in a DIA-type guide block system. Their pressure generation curve, however,  
89 indicated potential to generate even higher pressures at higher press load. Therefore, it  
90 is worthwhile to attempt generation of higher pressures even at ambient temperature.  
91 We also consider that there is a room to generate higher pressures more efficiently than  
92 Kunimoto et al. [10] by adopting the anvil tapering.

93         In this study, we attempted higher-pressure generation using DIA-type KMAs  
94 with TJS01 flat and tapered anvils up to a press load of 15 MN at temperatures of 300-  
95 2000 K. We compared pressure efficiencies between the flat and tapered second-stage  
96 anvils and discussed usefulness of anvil tapering.

97

## 98 **2. Experimental methods**

99         High-pressure-temperature experiments were conducted using KMAs,  
100 "SPEED-1500" [11] and "SPEED-*Mk.II*" [12] installed in the beam line BL04B1, at the  
101 synchrotron radiation facility SPring-8, Japan, which adopt the DIA-type guide block  
102 system and have a maximum press load of 15 MN. As mentioned above, the second-

103 stage anvils were made of TJS01 produced by Fuji Die Co., Ltd. Samples were  
104 compressed using the flat and 1°-tapered anvils with 1.0-mm and 1.5-mm truncations  
105 with SPEED-1500 and SPEED-*Mk.II*, respectively. We adopted the geometry of the  
106 tapered anvil used in Ishii et al. [9]. Although optimization of the taper angle may be  
107 important for high-pressure generation, it was empirically fixed to 1 degree in this  
108 study. A detailed design of the tapered anvil was described in Ishii et al. [9]. The reason  
109 why Kunimoto et al. [10] tested only to 10 MN is use of relatively small (14-mm edge  
110 length) second-stage anvils. This small anvil size limited applied press loads to avoid  
111 serious damage of first-stage anvils. We applied higher press loads up to 15 MN by  
112 employing the second-stage anvils with a 26-mm edge length.

113 Generated pressures were determined from the unit cell volume of Au by  
114 energy dispersive X-ray diffraction with the equation of state by Tsuchiya [13]. White  
115 X-ray beams were collimated to 50  $\mu\text{m}$  horizontally and 100  $\mu\text{m}$  vertically. Diffraction  
116 angles ( $2\theta$ ) were fixed to 6 and 8° for SPEED-1500 and SPEED-*Mk.II*, respectively.  
117 Diffracted X-rays were collected for 180-900 s using a germanium solid-state detector  
118 (SSD) in an energy range up to ca. 160 keV calibrated using fluorescence of Cu, Mo,  
119 Ag, Ta, Pt, Au and Pd. Samples were oscillated around the vertical axis between 0 and  
120 8° in the case of SPEED-*Mk.II* to suppress effects of grain growth [12]. Errors in  
121 pressures were typically 0.1-0.3 GPa and 0.5 GPa at most.

122 Figure 1 shows cross sections of cell assemblies for the flat and tapered WC  
123 anvils. Cr<sub>2</sub>O<sub>3</sub>-doped MgO octahedra with 4.1-mm and 5.7-mm edge lengths were used  
124 as pressure media, combining with the flat and tapered anvils, respectively. Figure 1a  
125 illustrates a cell assembly for the flat anvils. A starting material was a mixed powder of  
126 CaSnO<sub>3</sub> perovskite (pv) and Au with a weight ratio of 8:1. CaSnO<sub>3</sub> pv was synthesized  
127 by heating a mixture of CaCO<sub>3</sub> and SnO<sub>2</sub> with a mole ratio of 1.03:1 at 1300 K and  
128 ambient pressure for 24 h after decarbonation. A cylindrical TiB<sub>2</sub> + BN + AlN  
129 composite heater was put in the pressure medium, and electrically connected with two  
130 anvils using Re electrodes. The sample was located at the center of the furnace. LaCrO<sub>3</sub>  
131 discs were put at the both ends of the furnace for thermal insulation. The furnace and  
132 electrodes were filled with diamond powder. A cell assembly in Figure 1b has no  
133 furnace and was used for pressure generation at room temperature with the tapered  
134 anvils. An Au foil in MgO powder was put at the center part of the pressure medium for  
135 measurement of pressure. Dense Al<sub>2</sub>O<sub>3</sub> rods were placed at the both sides of the MgO +  
136 Au part. Figure 1c shows a cell assembly for pressure generation at high temperatures

137 with the tapered anvils. A sintered mixture of MgO and 10 wt.% of Au was synthesized  
138 at 2 GPa and 1300 K for 1 hour using a KMA, and was placed between dense Al<sub>2</sub>O<sub>3</sub>  
139 rods in a Mo foil heater. A LaCrO<sub>3</sub> sleeve was placed around the heater for thermal  
140 insulation. Mo electrodes were placed on the both ends of the heater. Al<sub>2</sub>O<sub>3</sub> X-ray  
141 windows of 0.5 mm in diameter were set along the X-ray path outside of the furnace  
142 (Figure. 1c-2). Temperature was measured using a W97%Re3%–W75%Re25%  
143 thermocouple. Pyrophyllite gaskets were put around the pressure medium. For the flat-  
144 anvil experiment, gaskets were baked at 1083 K for better pressure generation.

145 We conducted experiments with each cell assembly in the following way. In  
146 S3052, which is the flat-anvil experiment with the assembly of Figure 1a, the press load  
147 applied to the sample was increased at a constant rate. Compression was stopped every  
148 2-3 MN, and the sample was heated to 1100-1300 K, and then cooled to ambient  
149 temperature for relaxation of stress from the pressure medium and the gaskets.  
150 Diffraction patterns of the sample were taken before, during and after the heating at  
151 each press load. Heating was made at press loads up to 9 MN. In M1873, which is the  
152 ambient-temperature tapered-anvil experiment with the assembly of Figure 1b, the  
153 sample was compressed at a constant rate, and sample diffraction patterns were taken at  
154 intervals of 1-3 MN up to 15 MN. In M1904, which is the high-temperature tapered-  
155 anvil experiment with the assembly of Figure 1c, the sample was compressed to 15 MN  
156 with collecting diffraction patterns at intervals of 1-3 MN. At the highest press load,  
157 heating was conducted to 2000 K at a rate of 100 K/min with collecting diffraction  
158 patterns every 200-300 K. Another run (M1890) was also conducted using the assembly  
159 of Figure 1c. However, we tested high-pressure generation only at room temperature in  
160 the same way as M1904 because the temperature measurement with thermocouple was  
161 failed during compression.

162

### 163 **3. Results and discussion**

164 Table 1 summarizes experimental conditions of each run and results at 15 MN  
165 and 300 K.

166

#### 167 **3.1. High-pressure generation with flat anvils**

168 Figure 2 shows results of the pressure generation test with flat anvils. At room  
169 temperature, a pressure of 52.2 GPa was generated at a press load of 9 MN. A pressure  
170 of 54.0 GPa was achieved at 1100 K and the press load. In a heating-cooling cycle at

171 each press load, pressures increase and decrease by heating and cooling, respectively,  
172 due to thermal pressure. At press load above 9 MN, an increase rate of pressure  
173 generation becomes worse, and a pressure of only 53.6 GPa was generated even at the  
174 maximum press load of 15 MN and room temperature. Although sample pressures were  
175 expected to increase by heating, the sample was not heated because the anvil gap was  
176 already closed to 50  $\mu\text{m}$  at 9 MN, and we were afraid of complete closure of the anvil  
177 gap by heating at higher press load.

178

### 179 ***3.2 High-pressure generations with tapered anvils***

180 Figure 3 summarizes results of the pressure generation tests with the tapered  
181 anvils at room temperature. In all runs, we succeeded in generating pressures higher  
182 than 60 GPa at the maximum load of 15 MN. In M1873, the highest pressure of 64.3  
183 GPa was achieved with the cell assembly for room temperature (Figure 1b). In addition  
184 to usage of the hard tapered anvils, generation of such a high pressure may be due to a  
185 replacement of large volume of MgO pressure medium to alumina, which has higher  
186 bulk modulus than MgO, as discussed in Ishii et al. [9]. The pressure efficiency in  
187 M1873 is higher than those of the others especially below 12 MN. This is probably  
188 because the pressure medium for M1873 (Figure 1b) is replaced by less kinds of cell  
189 parts than that of the other runs (Figure 1c). Therefore, the internal filling rate for the  
190 cell assembly of M1873 would be higher, which may enhance the pressure efficiency  
191 because applied force is transmitted to the sample more efficiently. Figure 3 also shows  
192 pressures generated using TF05 tapered anvils with a hardness of  $H_v = 2200$ [9] for  
193 comparison. At 15 MN, pressure generated with the TJS01 tapered anvils (64 GPa) is by  
194 more than 20 GPa higher than that with the TF05 ones (43 GPa). This result clearly  
195 shows use of second-stage anvil with high hardness is very useful for pressure  
196 generation in KMA as discussed in previous studies (e.g. [9,10]). We also indicate  
197 usefulness of anvil tapering for pressure generation. The present results show the  
198 pressure generation with the tapered anvils up to 6 MN is relatively high or almost the  
199 same efficiency in comparison with that of the flat anvils, even though the tapered  
200 anvils adopted a larger anvil truncation (1.5 mm) than the flat ones (1.0 mm). Ishii et al.  
201 [9] compared pressure efficiencies between flat and tapered anvils with 1.5-mm  
202 truncation and showed anvil tapering enhances pressure efficiency even at 1 MN.  
203 Therefore, the present pressure efficiency difference was probably filled by anvil  
204 tapering. The pressure generation with the tapered anvils of 54-57 GPa was also by 2-5

205 GPa higher than that with the flat anvils at 9 MN. Additionally, the pressure-increasing  
206 rate with the flat anvils was only 0.2 GPa/MN at press loads above 9 MN, whereas that  
207 with tapered anvils was 1.5 GPa/MN. Thus, we have confirmed that the technique of  
208 anvil tapering is very effective for high-pressure generation especially at high press-  
209 load.

210 In M1904, the sample was heated to 2000 K at a press load of 15 MN (Figure  
211 4). Compared to the flat anvil experiment (Figure 2), pressure continuously decreased  
212 during heating to 2000 K. This is probably because of the less support for confining  
213 pressure caused by wider anvil gap than that of flat anvil. Although sample pressures  
214 drastically decreased with increasing temperature, pressures over 50 GPa were kept up  
215 to 1600 K, and it was still 48.0 GPa at 2000 K. The reason for the drastic pressure drop  
216 could be due to high heat flow from the heater through the Al<sub>2</sub>O<sub>3</sub> X-ray window, which  
217 has a thermal conductivity (~7 W/m·K at 1100 K and 1atm) higher than the LaCrO<sub>3</sub>  
218 thermal insulator (~2 W/m·K at 1100 K and 1 atm) [14]. We need to improve the high-  
219 temperature generation technique to suppress the large pressure drop. Nevertheless, we  
220 emphasize that the maximum pressure generated using KMAs with the WC anvils was  
221 44 GPa at high temperatures of 2000 K, which was achieved by the present author's  
222 previous work [9]. Since generated pressure by an assembly with X-ray windows can  
223 generate much lower pressure than that without X-ray windows [9], it is expected that  
224 much higher pressures than 48 GPa can be generated at temperatures around 2000 K by  
225 using the cell assembly without X-ray windows.

226 It is noted that the tapered geometry held an anvil gap of ~200 μm even at 15  
227 MN (Figure 5b), which allows efficient collection of X-ray diffraction at such high  
228 press loads. Kunimoto et al. [10] measured surface undulation of 1.5-mm truncation  
229 anvils, which was caused by plastic deformation during compression. They showed that  
230 the hinder parts at ~3 mm backward from the truncation are raised by 10-20 μm with the  
231 depression (40-80 μm) near the truncated surface, depending on hardness of second-  
232 stage WC anvil and applied press load. Under load, such undulation should become  
233 larger because of elastic deformation. Figures 6a and 6b, respectively, show schematic  
234 cross sections of flat and tapered anvils deformed by stress from confining pressure. As  
235 shown in Figure 6a, the surface deformation in the flat-anvil experiment would prevent  
236 a part of X-ray from going through the anvil gap. On the other hand, the tapered anvil  
237 geometry can avoid the closure because the backside of the truncation is originally  
238 lower than the anvil top.



239 In the present experiments, blow-outs occurred every time during  
240 decompression and all anvils were broken. Although one of the reasons would be  
241 because of too-short decompression time (2-3 hours) due to limited time in synchrotron  
242 experiment, this may be able to be suppressed by further optimization of cell assembly,  
243 gasket size and anvil geometry.

244 As a conclusion, our high-pressure generation technique will allow us studying  
245 material properties under conditions corresponding to the upper part of the lower mantle  
246 (1200 km) without the SD anvils. Especially, this technique will facilitate investigation  
247 of phase relations, physical and chemical properties in lower mantle minerals such as  
248 bridgmanite (e.g. elasticity, diffusivities of each atom and spin state of Fe), which will  
249 improve models of structure and dynamics in the lower mantle. It will be also expected  
250 to be applied for synthesis of novel material under extremely high pressure.

251

## 252 **Acknowledgements**

253 The synchrotron radiation experiments were performed at the BL04B1 of  
254 SPring-8 with the approval of the Japan Synchrotron Radiation Research Institute  
255 (JASRI) (Proposal Nos. 2015B1319, 2015B1504, 2015B1761, 2016A1172, and  
256 2016A1434). This study is also supported by the research project approved by DFG  
257 (KA-3434/7, KA-3434/8 and KA-3434/9) and BMBF (05K16WC2) to T. Katsura. and  
258 by the Overseas Research Fellowship from the Scientific Research of the Japan Society  
259 for the Promotion of Science (JSPS) for Young Scientists to T. I.

260

## 261 **References**

- 262 [1] Kawai N, Endo S. The generation of ultrahigh hydrostatic pressure by a split sphere  
263 apparatus. *Rev Sci Instrum.* 1970;4:425-428.
- 264 [2] Keppeler H, Frost D. Introduction to minerals under extreme conditions. In: Miletich  
265 R, editor. *Mineral Behavior at Extreme Conditions*. Budapest: Eötvös University Press;  
266 2005. p. 1-30.
- 267 [3] Tange Y, Irifune T, Funakoshi K. Pressure generation to 80 GPa using multianvil  
268 apparatus with sintered diamond anvils. *High Press Res.* 2008; 28: 245-254.
- 269 [4] Katsura T, Yokoshi S, Kawabe K, et al. *P-V-T* relations of MgSiO<sub>3</sub> perovskite  
270 determined by *in situ* X-ray diffraction using a large-volume high-pressure apparatus.  
271 *Geophys Res Lett.* 2009;36:L01305(1-6).
- 272 [5] Wang F, Tange Y, Irifune T, et al. *P-V-T* equation of state of stishovite up to mid-

- 273 lower mantle conditions. *J Geophys Res.* 2012;117:B06209(1-11).
- 274 [6] Yamazaki D, Ito E, Yoshino T, et al. Over 1Mbar generation in the Kawai-type  
275 multianvil apparatus and its application to compression of  $(\text{Mg}_{0.92}\text{Fe}_{0.08})\text{SiO}_3$  perovskite  
276 and stishovite. *Phys Earth Planet Inter.* 2014; 228: 262-267.
- 277 [7] Irifune T, Kuroda K, Funamori N, et al. Amorphization of Serpentine at high  
278 pressure and high temperature. *Science.* 1996; 272: 1468-1470.
- 279 [8] Ito E, Kubo A, Katsura T, Akaogi M, et al. High pressure transformation of pyrope  
280  $(\text{Mg}_3\text{Al}_2\text{Si}_3\text{O}_{12})$  in a sintered diamond cubic anvil assembly. *Geophys Res Lett.* 1998;  
281 25: 821-824.
- 282 [9] Ishii T, Shi L, Huang R, et al. Generation of pressures over 40 GPa using Kawai-  
283 type multi-anvil press with tungsten carbide anvils. *Rev Sci Instrum.* 2016; 87:  
284 024501(1-6).
- 285 [10] Kunimoto T, Irifune T, Tange Y, et al. Pressure generation to 50 GPa in Kawai-type  
286 multianvil apparatus using newly developed tungsten carbide anvils. *High Press Res.*  
287 2016; 36: 1-8.
- 288 [11] Utsumi W, Funakoshi K, Urakawa S, et al. SPring-8 beamlines for high pressure  
289 science with multianvil apparatus. *Rev. High Press Sci Technol.* 1998; 7: 1484-1486.
- 290 [12] Katsura T, Funakoshi K, Kubo A, et al. A large-volume high-pressure and high-  
291 temperature apparatus for *in situ* X-ray observation, 'SPEED-Mk.II'. *Phys Earth Planet*  
292 *Inter.* 2004; 143-144: 497-506.
- 293 [13] Tsuchiya T. First-principles prediction of the  $P$ - $V$ - $T$  equation of state of gold and  
294 the 660-km discontinuity in Earth's mantle. *J Geophys Res.* 2003;108:2462 (ECV1-9).
- 295 [14] Kingery W. D., Francl J., Coble R. L., e al. Thermal conductivity: X, data for  
296 several pure oxide materials corrected to zero porosity. *Journal of the American*  
297 *Ceramic Society*, 1954; 37: 107-110.

298

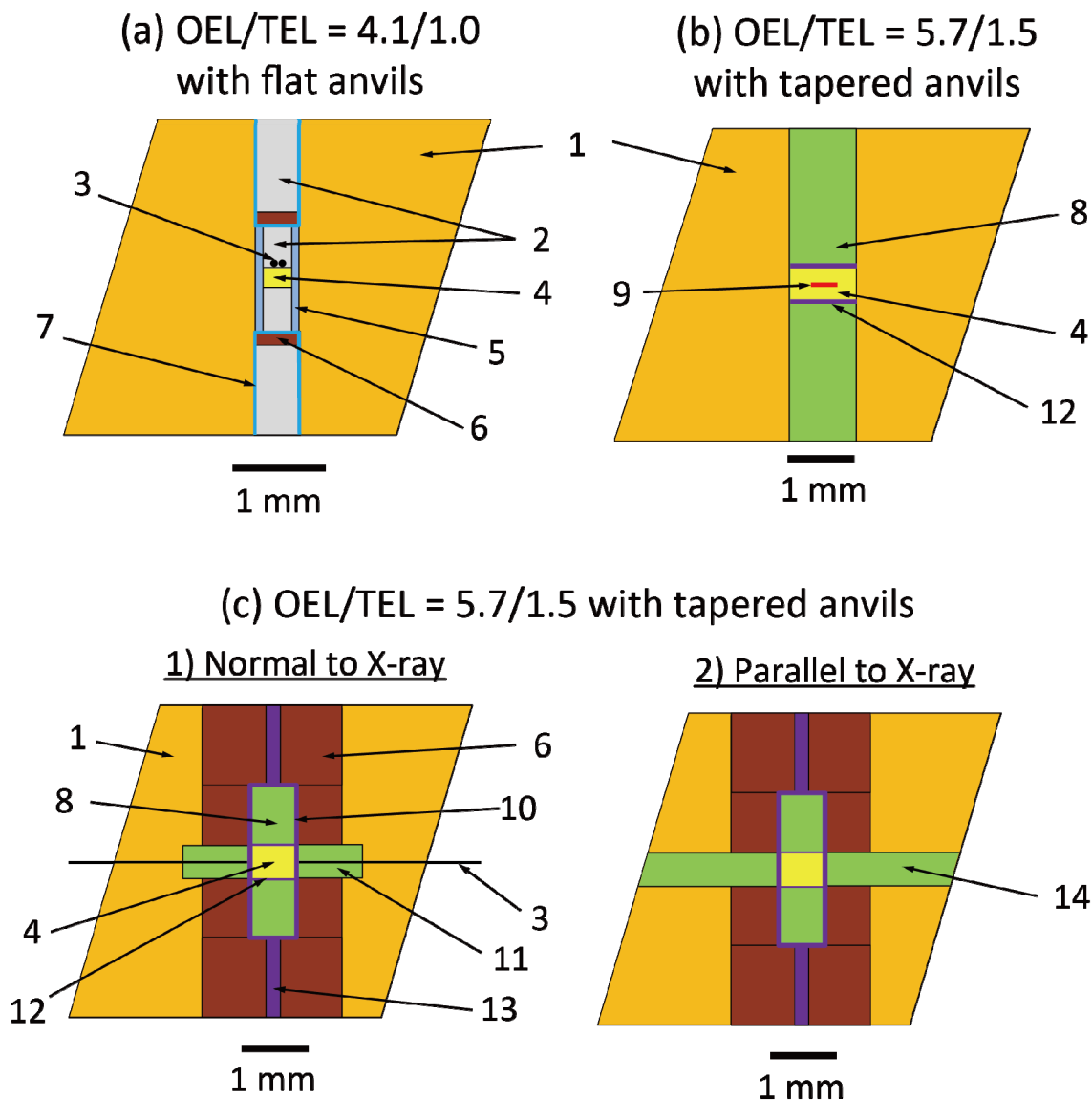
299 Table 1. Experimental conditions and results at 15 MN and 300 K.

300	Run no.	KMA	OEL/TEL	Anvil geometry	Cell assembly	$P$ (GPa)
301	S3052	SPEED-1500	4.1/1.0	flat	Fig. 1a	53.6
302	M1873	SPEED-Mk.II	5.7/1.5	tapered	Fig. 1b	64.3
303	M1890	SPEED-Mk.II	5.7/1.5	tapered	Fig. 1c	63.3
304	M1904	SPEED-Mk.II	5.7/1.5	tapered	Fig. 1c	62.4

305 KMA, Kawai-type multi-anvil apparatus; OEL, octahedral edge length of pressure  
306 medium; TEL, truncated edge length of second-stage anvil.

307

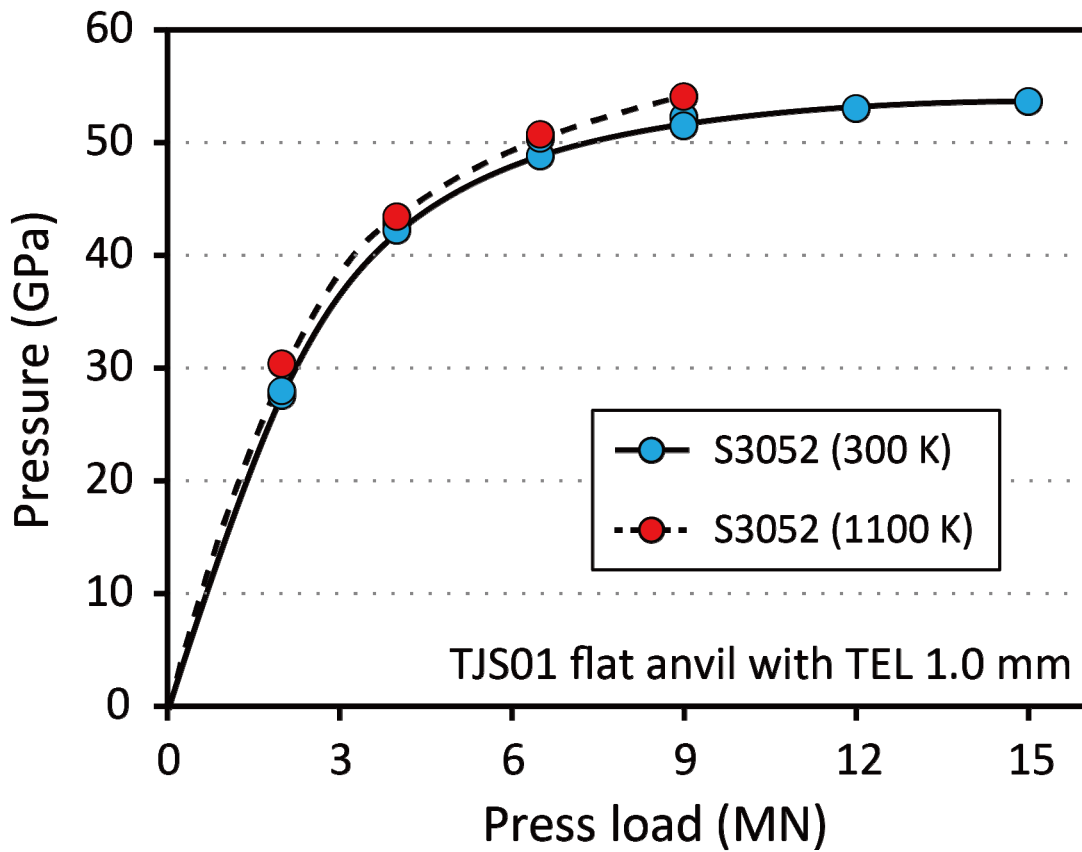
308 **Figure captions**



309

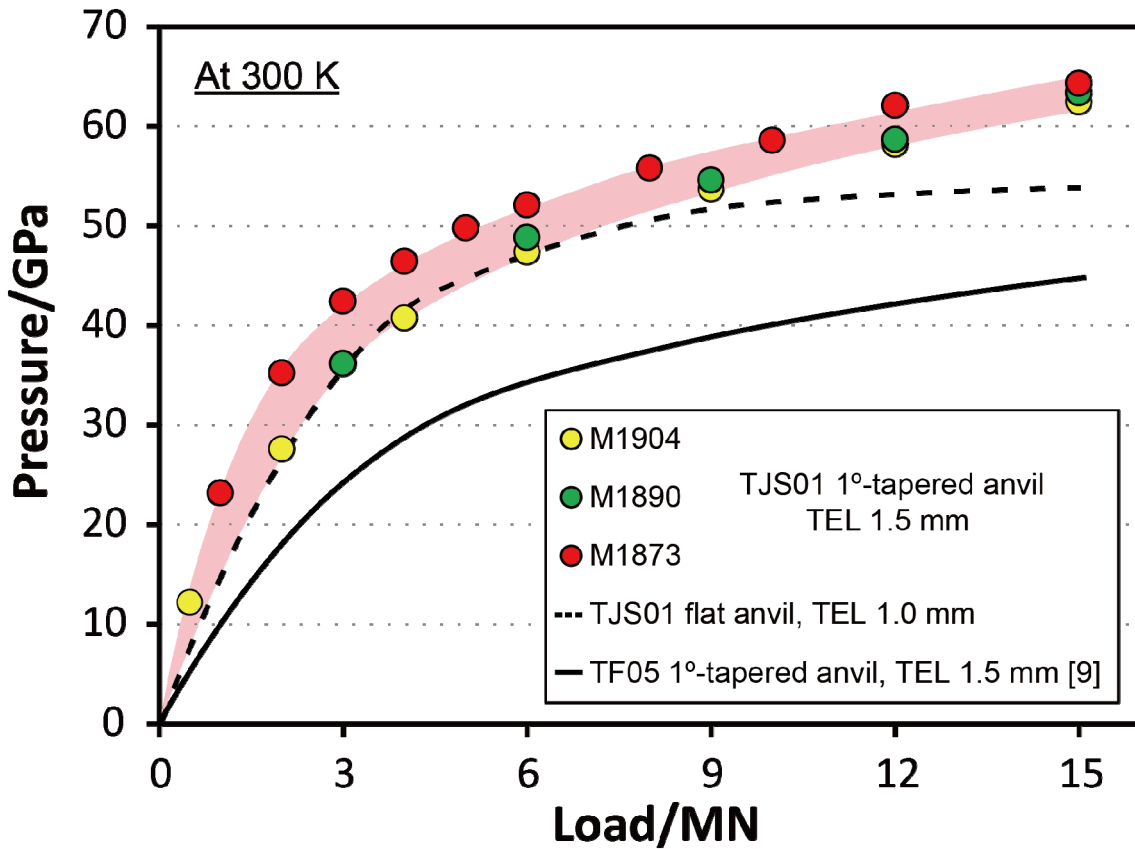
310 Figure 1. Cross sections of cell assemblies combined with (a) flat anvils with 1.0-mm  
311 truncation, (b) and (c) 1°-tapered anvils with 1.5-mm truncation for pressure generation  
312 tests at room temperature and high temperature, respectively. 1, 5 wt.% Cr<sub>2</sub>O<sub>3</sub>-doped  
313 MgO pressure medium; 2, diamond powder; 3, W97%Re3%-W75%Re25%  
314 thermocouple; 4, sample; 5, TiB<sub>2</sub>+BN+AlN composite heater; 6, LaCrO<sub>3</sub> thermal  
315 insulator; 7, Re electrode; 8, dense alumina; 9, Au foil; 10, Mo heater; 11, dense  
316 alumina electrical insulator for the thermocouple; 12, Mo disc; 13, Mo electrode; 14,  
317 dense alumina X-ray window. OEL, octahedral edge length of pressure medium; TEL,

318 truncated edge length of second-stage anvil.



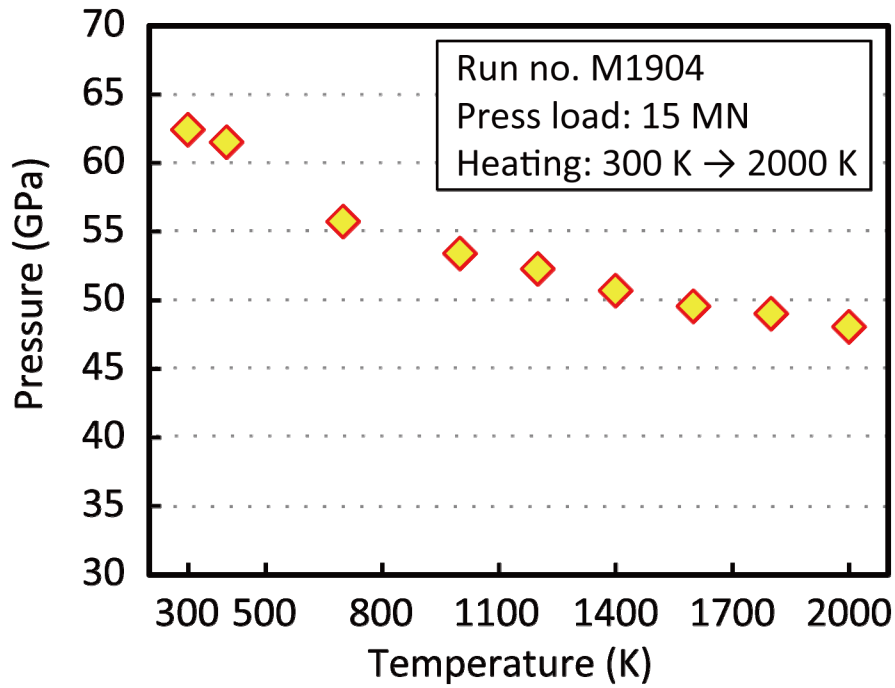
319

320 Figure 2. Results of a pressure generation test (S3052) in the KMA using TJS01 flat  
321 anvils with 1.0-mm truncation. Pressures at 300 K were measured before and after  
322 heating up to 9 MN.



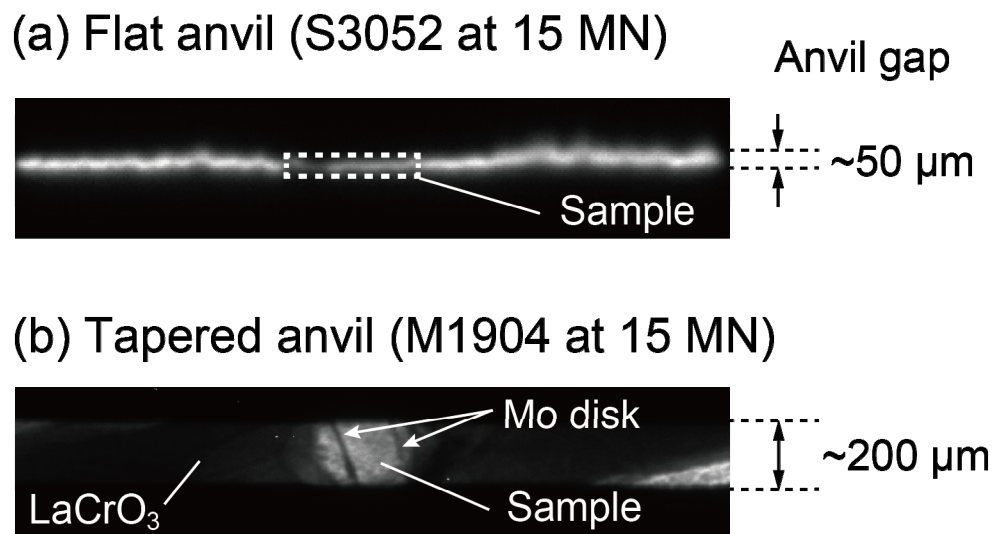
323

324 Figure 3. Results of pressure generation tests in the KMA using TJS01 tapered anvil  
325 with 1.5-mm truncation. Band-like curve indicates a region of pressure generation with  
326 the TJS01 tapered anvils. Dashed curve represents pressure generation using the TJS01  
327 flat anvils with 1.0-mm truncation in the present study (see Figure 2). Solid curve  
328 represents pressure generation using the TF05 1°-tapered anvils with 1.5-mm truncation  
329 reported by Ishii et al. [9]. TEL, truncated edge length.



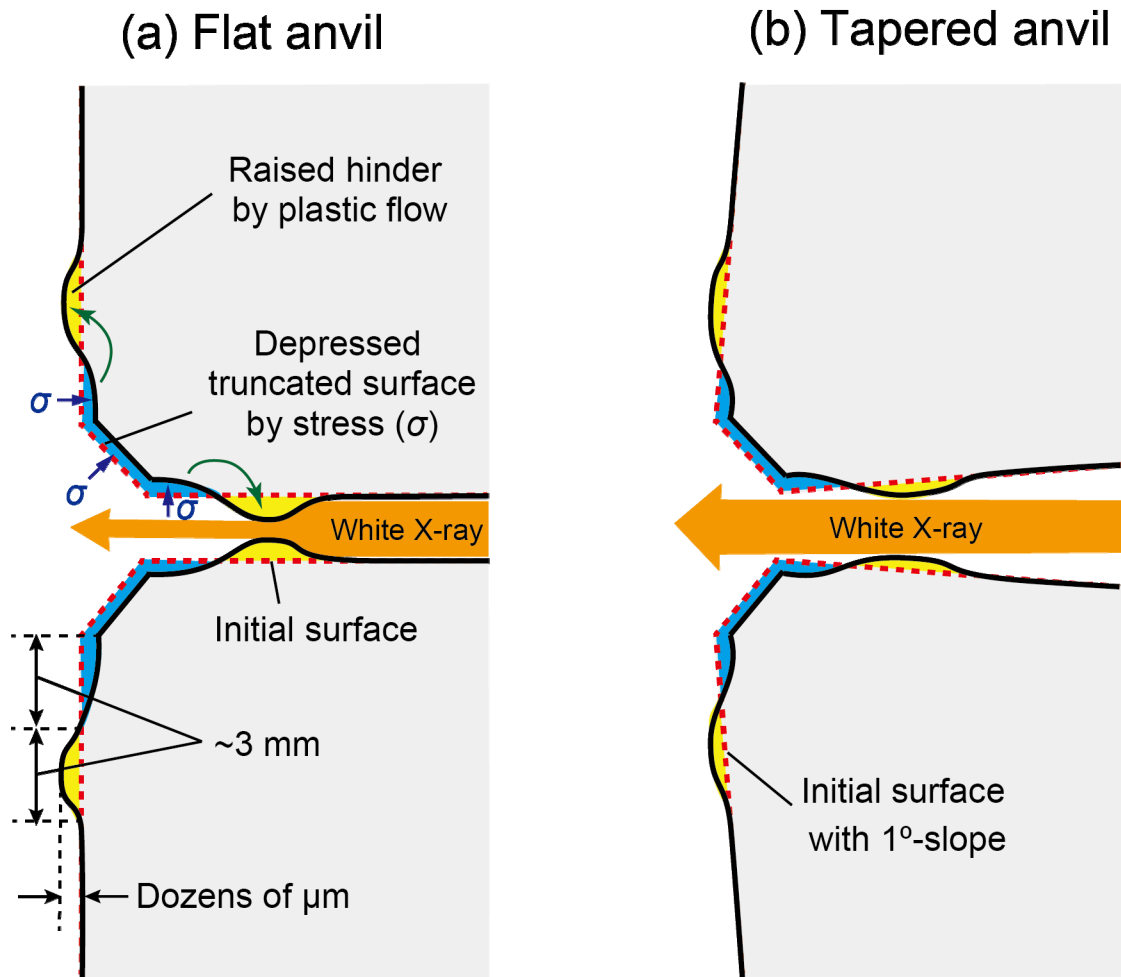
330

331 Figure 4. Pressure generations in the KMA with TJS01 tapered anvils during heating up  
332 to 2000 K in M1904.



333

334 Figure 5. X-ray radiographic images of anvil gaps for (a) the flat and (b) tapered anvils  
335 at a press load of 15 MN and room temperature.



336

337 Figure 6. Deformations of (a) flat and (b) tapered anvil surfaces caused by stress from  
338 confining pressure. Dashed and solid lines represent initial and deformed surfaces,  
339 respectively. Small blue arrows indicate the simplified stress ( $\sigma$ ) from confining  
340 pressure. The deformation of anvil top raises the hinder part by dozens of micrometers  
341 due to the plastic flow (green arrows).